Journal of Molecular Catalysis A: Chemical 313 (2009) 7–13

Contents lists available at ScienceDirect

Journal of Molecular Catalysis A: Chemical

journal homepage: www.elsevier.com/locate/molcata

Codiffusion and counterdiffusion of para-xylene and ortho-xylene in a zeolite with 10 MR/12 MR interconnected channels. An example of molecular traffic control

R. Roque-Malherbe[a,*], V. Ivanov[b,1]

[a] Institute for Physical Chemical Applied Research, School of Science, University of Turabo, PO Box 3030, Gurabo, PR 00778-3030, USA
[b] Rohm and Haas, Bolshaya Akademicheskaya Ulitza, 5A, 5th floor, Moscow 125299, Russia

ARTICLE INFO

Article history:
Received 13 April 2009
Received in revised form 10 July 2009
Accepted 16 July 2009
Available online 23 July 2009

Keywords:
Diffusion
Codiffusion
Counterdifusion
Xylenes
Molecular traffic control
CIT-1

ABSTRACT

Diffusion has a significant effect in zeolite catalysis. Molecular traffic control is a good example. For the study of diffusion in microporous crystalline materials with 10 MR/12 MR interconnected channels, as H-CIT-1, the isomers, para- and ortho-xylene are excellent probes. In this regard, by means of a FTIR technique, codiffusion and counterdiffusion of these isomers were studied. The values of the diffusivities in the codiffusion and counterdiffusion experiments were measured. A correlation in the transport of both isomers, during codiffusion and counterdiffusion was observed. Throughout codiffusion, the more mobile p-xylene molecule hinders the motion of o-xylene. During the counterdiffusion case, when p-xylene diffuses "in" and o-xylene "out" the zeolite, the 10 MR channels, which are blocked for the o-xylene molecules, are free for p-xylene motion. Subsequently, under the experimental conditions of the present study, molecular traffic control, takes place.

1. Introduction

Zeolites are crystalline, inorganic, microporous materials with frameworks composed of channels and cavities with pore and cavity windows dimensions normally smaller than 1 nm. In the application of zeolites, and other crystalline microporous materials, diffusion is a key effect [1–16]. Since, in numerous applications of these materials, molecular transport has a significant role in determining the overall process [3]. Nevertheless, diffusion in microporous crystalline materials is insufficiently understood. In this process, the structure of the transported molecules, its dimensions, the conformation of the zeolite pores and cavities, and the interactions of the diffusing molecules with the zeolite framework components plays an intricate role [1,2]. That is, in this confined situation, the motion of the molecules is governed by the geometry of the zeolite framework, which gives the force field background for diffusion [13].

In, adsorption, ion exchange, and catalysis, the constrained environment provided by a microporous crystalline material to a molecule or ion, moving inside its framework, can be applied to distinguish between different molecules or ions, and promote particular transition states using shape or size as selection criteria [17].

In a catalytic study of zeolites exhibiting structures where the 10-MR (member ring) and 12-MR channel intersects, was shown that, the catalytic behavior is strongly influenced by the void space left in the crossing points [18]. Besides, in a multicomponent diffusion system consisting of large coadsorbed molecules combined with smaller molecules the larger molecules traps the smaller ones in the zeolite channels [12]. These two previous examples are illustrations of the role of the dimensions of the zeolite and the molecules diffusing inside the zeolite in processes, such as, catalysis and separation, occurring within the zeolite.

The perception of reactivity enhancement by molecular traffic control (MTC) is related with the previously described effects [19]. The concept MTC describes an effect in chemical reactions, in microporous crystalline materials with porous systems showing different dimensions, where the reactant and product molecules choose dissimilar paths for diffusion [20]. That is, in particular circumstances, a binary mixture of molecules with diverse dimensions, diffusing in a framework structure exhibiting two pores with different widths can shows a divergence in the paths of the two diffusing molecules [21].

After years of debates, with the help of simulations, the possibility of MTC has been demonstrated [20,22–24]. However,

* Corresponding author. Tel.: +1 787 743 7979x4260; fax: +1 787 743 4114.
E-mail addresses: RRoque@suagm.edu, RRoquemalh@aol.com (R. Roque-Malherbe), 7617428@mail.ru (V. Ivanov).
[1] Tel.: +7 495 761 7428; fax: +7 495 125 54 03.

1381-1169/$ – see front matter © 2009 Elsevier B.V. All rights reserved.
doi:10.1016/j.molcata.2009.07.015

notwithstanding, the soundness of simulations; it is also necessary to give further experimental proofs to the MTC effect. Multicomponent diffusion in zeolites could help in this endeavor. In this regard, the diffusion of molecules through the pores of a zeolite with a structure exhibiting two pores with different widths could be applied to get experimental evidence of MTC. To provide this experimental support a zeolite with 10 MR/12 MR interconnected channels, is a very promising system [7]. Additionally, zeolites with 10 MR and 12 MR are of interest in industrial applications [24–27], because of their pore size, which give rise to shape selectivity and confinement effects [17,18,28]. Thereafter, for the application of these zeolites as catalysts, the study of mixture diffusion is very useful.

CIT-1, exhibiting the framework type CON [29], shows an especially attractive framework, since it is a microporous crystalline material with a channel system composed of 10 and 12 member rings [29–35]. SSZ-33, SSZ-26, and CIT-1, were the first of all described zeolites showing a framework containing a pore system shaped by crossed over 10 MR and 12 MR channels, giving access to the pore system, by means of both type of pores [31–35]. CIT-1, as the rest of the previously mentioned zeolites, can be considered as a component of a type of disordered materials, in which, the two end components, symbolized as polymorphs A and B, are structured by an identical periodic building unit, showing a different stacking sequence [30]. The frameworks which are shaped by the *ABAB*... stacking sequence are compatible with the polymorph A showing an orthorhombic symmetry [31,34]. Those structured by the *ABCABC*... stacking sequence match with polymorph B, which have a monoclinic symmetry [31,34]. The CIT-1 material corresponds to the pure polymorph B [36].

The zeolite CIT-1 shows a multidirectional channel system, composed of a 10 MR channel with an opening ring of, 0.51 nm × 0.45 nm, which is parallel to the [0 1 0] crystalline direction and two 12 MR channels [29]. One of these 12 MR channels, parallel to the [0 0 1] crystalline direction, has an opening ring of, 0.65 nm × 0.70 nm [29]. The other, with an opening ring of, 0.70 nm × 0.59 nm, is parallel to the [1 0 0] crystalline direction [29]. These channels intersects, approximately, every 1.0 nm or 1.5 nm, depending on the direction [7].

Owing to the diffusion critical diameter of xylenes (σ_m), that is, for para-xylene, σ_m = 0.58 nm, and for ortho-xylene, σ_m = 0.7 nm [1]; they are good probes for testing the intracrystalline transport of hydrocarbons in zeolites with 10 MR and 12 MR [5–9], as CIT-1. Consequently, in the present research, the codiffusion and counterdiffusion diffusivities of p-xylene and o-xylene mixtures within the pores of CIT-1 zeolite, have been measured by means of a FTIR technique [4–8], in order to get experimental proofs, related with the molecular traffic control effect.

2. Experimental

2.1. Materials

Zeolite B-CIT-1 was provided by R. Lobos [31–35]. To determine the crystallinity of the solids, X-ray powder diffraction (Cu Kα radiation) was applied. With a Philips diffractometer model PW 1710, equipped with graphite monochromator and scintillation counter, the measurements were carried out. The results indicated that the crystallinity of all the samples was near to 100%. To determine crystal size and morphology of the samples, scanning electron microscopy (SEM, JEOL-ISM 6300) was performed. For CIT-1 zeolite, spherical shaped crystals with average diameter of 1.5 μm were found.

For the removal of tetrahedral framework boron and insertion of aluminum in B-CIT-1 the corresponding calcined borosilicate was exchanged with a 2% (w/w) water solution of $Al(NO_3)_3$ at 100 °C [33]. Samples H-Al-CIT-1 (that is: H-CIT-1) are hence produced. By chemical analysis using atomic absorption (Varian SpectrAA 10 Plus), the chemical composition of the zeolite sample was tested. Then, for H-CIT-1, the measured bulk Si/Al ratio was 35.

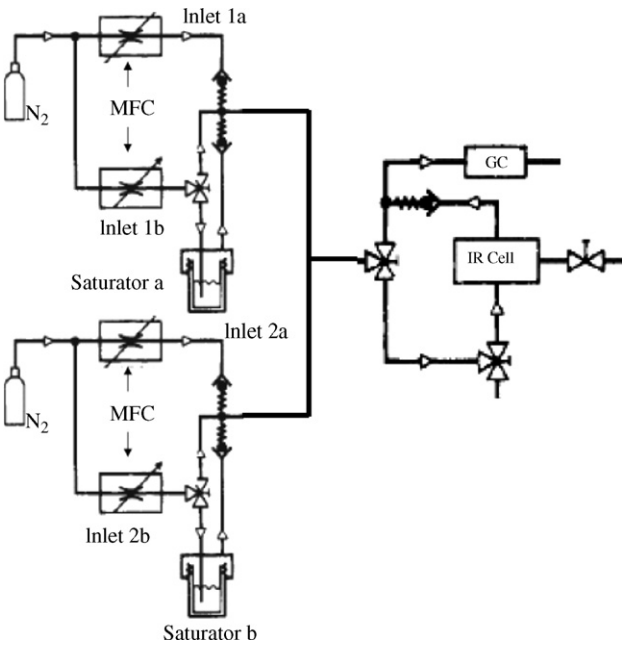

Fig. 1. Schematic representation of the experimental facility applied to perform adsorption kinetics measurements with the FTIR method.

The tested xylenes, i.e., para-xylene and ortho-xylene (Aldrich) were all analytical grade reagents and were further dehydrated using zeolite 4A.

2.2. Methods

2.2.1. Equipment

The equipment applied to make the diffusion studies is composed of an IR high temperature cell connected through stainless steel pipes to two manifolds containing two thermo stated saturators (see Fig. 1). For the carrier gas, nitrogen in our case [5–8], with grade of purity of 99.99%, both manifolds have two gas inlets. Throughout inlet 1b, the carrier gas bubbles through the saturator "a", in which one of the adsorbates is located. The carrier gas coming from the saturator "a" outlet, saturated with the corresponding hydrocarbon, is mixed with a measured flow of pure carrier gas, from inlet 1a. In both inlets, sensitive mass flow controllers (MFC) were located (see Fig. 1). By the simultaneous variations of both flow controls, the relative partial pressure of the hydrocarbon, in the range: $0.01 < P/P_0 < 0.9$, was controlled. Additionally, in the system, in order to measure the gas mixture composition, a gas chromatograph (FISONS 8000) was included [6].

2.2.2. Measurement methodology

In both stainless steel saturators, the xylenes to be tested were loaded. Both saturators were held at 25 °C. The flow of the gas carrier was divided in two, and through a flow controller, each of these streams were passed [6]. One stream went through the saturator, where the carrier gas bubbled in the liquid adsorbate. Thereafter, the gas flow, saturated with the substance under test, was mixed with the supplementary stream of pure carrier gas at the outlet of the saturator. After that, through the IR cell, the unified stream was passed [6]. Then, by monitoring the change in the intensity of an

IR peak, with a FTIR spectrometer, the measurement process is carried out. That is, the absorbance of a band of the sorbate molecule is measured. The FTIR spectrometer was a BIO RAD, FTS 40A. This equipment has a resolution of 8 cm^{-1}. The FTIR system was controlled by the BIO RAD WIN IR software, in the mode of advanced scan menu-kinetics. This software, depending of the kinetics of the sorption process, allowed us to store 400–1000 spectra (1 scan per spectrum, 0.85 s per scan, without delay between scans) [5]. To get the adsorption kinetic data, the range from 1480 to 1550 cm^{-1} and the band around 1517 cm^{-1} for p-xylene, and the double peak with bands at 1467 and 1497 cm^{-1} and the range from 1420 to 1520 cm^{-1} for o-xylene were measured [6].

The water-cooled, commercial AABSPEC, IR high temperature cell is the key equipment in the testing facility (see Fig. 1 [5,6]). To minimize leaking, in the cell, the demountable parts are fitted with Viton O-rings. The temperature of the sample holder is controlled electronically with very low variation of temperature, normally $\Delta T < 1\,^{\circ}C$ [5–8].

Self-supported wafers, obtained by pressing, 8 mg/cm^2, of the zeolite sample powder at 400 MPa, are placed in the sample holder and introduced in the cell.

Prior to the measurement of the diffusion coefficient, in a flow of the pure carrier gas, the samples under test are carefully degassed at 723 K, during 2 h. Thereafter, the sample is cooled to the desired temperature and kept at this temperature with the help of the temperature control. As a reference, a background spectrum of the pure degassed zeolite is obtained. After that, at a precisely defined pressure, the flow coming from the saturator, after mixing with the flow of pure carrier gas, is admitted to the IR cell. During the codiffusion and counterdiffusion experiments, with the gas chromatograph the composition ($C_{p\text{-}x}$ and $C_{o\text{-}x}$) of the final hydrocarbon mixture was measured [6].

By the combination of the flow of the pure carrier gas (200 ml/min each) with the flows coming from saturators a (p-xylene) and b (o-xylene), the codiffusion experiments, were performed. To get the desired relative partial pressure both flow rates were adjusted. Thereafter, a series of experiments at one temperature (400 K) and different, compositions ($C_{p\text{-}x}$ (%) = 10, 20, 50, 75, 90 and 100%), were performed. It is necessary to recognize that the zeolite load with both isomer molecules is the same for the different compositions, that is, the total number of both isomer molecules is conserved. Additionally, experiments at different temperatures and $C_{p\text{-}x}$ = 50% were also carried out.

To accumulate the kinetic data, at the moment of the admittance of the mixture of p-xylene plus o-xylene, the collection of the set of IR spectra, was started. The obtained spectra were saved in the computer memory. Thereafter, the increase with time of the bands corresponding to both p-xylene and o-xylene, were measured with the help of the BIO RAD WIN IR software.

In the counterdiffusion experiment, the sample was initially saturated with a stream of o-xylene (for p+o-xylene counterdiffusion) or p-xylene (for o+p-xylene counterdiffusion), at a partial pressure of 6.7 Pa. To this stream of carrier gas, p-xylene, for the p+o-xylene counterdiffusion, or o-xylene, for o+p-xylene counterdiffusion, were respectively admitted. Thereafter, the same partial pressures, 6.7 Pa for both hydrocarbons were attained, to get, $C_{p\text{-}x} = C_{o\text{-}x}$ = 50%. At the moment of the admittance of p-xylene (for p+o-xylene counterdiffusion) or o-xylene (for o+p-xylene counterdiffusion), the collection of the set of IR spectra, was started. Thereafter, the increase of the band corresponding to p-xylene (for p+o-xylene counterdiffusion) or o-xylene (for o+p-xylene counterdiffusion) was measured [6].

Finally, the intensities of the bands in the spectra corresponding to the gaseous hydrocarbon phase were checked. The measured intensities were negligible in comparison with the measured bands of the adsorbed para- and ortho-xylene [5–8].

2.2.3. Methodology for the calculation of diffusivities

For the description of the transport process of one component in zeolites, the main parameter is the transport diffusion coefficient [16]. This parameter is also named, Fickean diffusion coefficient or chemical diffusion coefficient (D) [1–3,15]. With the help of a solution of Fick's second law, this parameter is measured [37]. A particular solution of the Fick's second law, for a spherical geometry, with variable surface concentration, and initial concentration inside the sphere equal zero, appropriate for the experimental setup used here, is applied. That is [37]:

$$\frac{M_t}{M_\infty} = 1 - 3\frac{D}{\beta r^2}\exp(-\beta t)\left\{1 - \left(\frac{\beta r^2}{D}\right)^{1/2}\cot\left(\frac{\beta r^2}{D}\right)^{1/2}\right\} + \left(\frac{6\beta r^2}{D\pi^2}\right)\sum_1^\infty\left(\frac{\exp((-Dn^2\pi^2 t)/r^2)}{n^2[n^2\pi^2 - ((\beta r^2)/D)]}\right) \quad (1)$$

where $M_t \propto A_t$ and $P = P_0[1 - \exp(-\beta t)]$, where, P_0, is the steady-state partial pressure, and, P, is the partial pressure at time, t, in the cell. Consequently, the initial non-stationary partial pressure of the sorbate in the gas stream is accounted for with the help of the parameter, β.

Cutting the series in Eq. (1), and using only the first four terms, an accurate approximation is obtained. With the help of a non-linear regression process, i.e., the Levenberg-Marquardt iterative fitting algorithm, the experimental data can be numerically fitted to this approximation. With the help of the Peakfit® computer program, this process is performed [38].

When diffusion occurs in spherical particles of radius "$r = a/2$", as is the case for the diffusion in the H-CIT-1 zeolite, the use of Eq. (1) is justified. Indeed, this zeolite shows spherical shape crystals with a diameter: $a = 1.5 \pm 0.1$ μm, where the reported error: ±0.1 μm, takes into account the particle size distribution of the studied sample.

In the interpretation of the uptake data, additional transport mechanisms superimposed on the intracrystalline diffusion are not considered [16,39]; i.e., we are measuring diffusion in the zeolite crystals. This fact implies the absence of macroporous limitations for the transport of the diffusing molecules, during the sorption process, in the wafers included in the IR cell [4,5,16]. This condition is valid, because the zeolite wafers are very thin, and completely surrounded by a fast flow of the gas mixture. Additionally, the diffusion coefficient was considered approximately constant. This condition is valid because all the experiments were carried out at low coverage.

The previously described experimental conditions allow the application of Eq. (1), to fit the experimental data, in order to calculate the single component Fickean diffusion coefficient [2,3,5,7,8]. For the evaluation of the diffusivities in the case of codiffusion and counterdiffusion, the methodology above described, adapted for binary diffusion, as will be explained in Section 3.2, was applied [6].

3. Results and discussion

3.1. Acid sites in the tested H-CIT-1 sample

In Fig. 2, the IR spectra of the dehydrated H-CIT-1, in the OH region is reported. It can be seen, that the, Si–OH–Al, bridged hydroxyl groups, in the H-CIT-1 sample appears at 3615 cm^{-1}, and the intensity of the band is much lower than those reported in more acid zeolites such as H-ZSM-5 [5] and H-ZSM-11 [6]. On the other hand, the silanol groups in the H-CIT-1 sample, appears at about: 3734 cm^{-1} and the intensity of the band is high. The: Si–OH–Al, bridged hydroxyl groups are Broensted acid sites. Conversely, silanols, which appears in the region around 3750 and

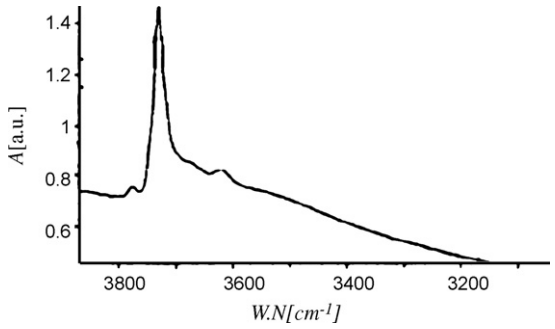

Fig. 2. FTIR spectrum of the dehydrated H-CIT-1 zeolite in the OH region: absorbance (*A*) versus wave number (*W.N.*).

3700 cm^{-1} are not acidic. From this spectrum, is possible to understand, that the tested sample has a small number of acid sites.

3.2. Codiffusion and counterdiffusion of p-xylene and o-xylene in a zeolite with 10 MR/12 MR interconnected channels

When a molecule is transported, within the channels and/or cavities of a microporous crystalline material, it becomes attracted to and repelled by different forces created by a group of interactions, such as: dispersion, repulsion, polarization, field dipole, field gradient quadrupole, sorbate–sorbate, and acid–base interactions [2]. In some cases, it is feasible to consider that the adsorbate–adsorbent interaction field within these structures is characterized by the presence of sites of minimum potential energy. Then, it is possible to suppose, that this transport process can be described as an activated molecular hopping between fixed sites [1–3,5,40,41].

For para- and ortho-xylene the principal interactions of the molecules with a zeolite framework are the acid–base interaction and the dispersion and repulsion interactions between the molecule and the zeolite framework [6,26].

In acid zeolites, protons are coordinated with negatively charged oxygen atoms surrounding aluminium atoms [42]. These arrangement forms Broensted acid sites. The acid–base interaction between the zeolite acid sites (Z-OH) and both xylenes molecules (B); could be represented by the following expression [43]:

$$Z\text{–}OH(s) + B(g) \rightarrow ZO^{\delta-} \ldots HB^{\delta+}(s)$$

Consequently, for a more basic molecule adsorbed in the same acid site, the interaction will be stronger. Thereafter, since, the relative basicity for para and ortho-xylene is 1.00 and 1.13, respectively [44]. Thus, o-xylene will be more strongly adsorbed than p-xylene. However, given that the intensity of the band corresponding to the bridged hydroxyl groups in the studied H-CIT-1 sample is very low; then, in the studied sample are only present a small amount of acid sites, to have a noteworthy influence in the diffusion mechanism.

With respect to the dispersion and repulsion interactions, the p-xylene molecular diffusion critical diameter is $\sigma_m = 0.58$ nm [1,5], and σ_w, the maximum window or channel diameter of the zeolite is [41] $\sigma_w = 0.51$ nm, for the 10 MR channel and $\sigma_w = 0.70$ nm for the 12 MR channels [29]. Subsequently, since the interaction of hydrocarbons with the zeolite pores strongly depends on its relative sizes [28,45], it is possible to state that p-xylene should freely moves throughout the 12 MR pores of the H-CIT-1 framework and relatively free through the 10 MR channels. This statement is based on experimental data previously obtained for single component p-xylene diffusion in ZSM-11 (a zeolite showing an intersecting two-directional system of 10 MR channels with: $\sigma_w = 0.58$ nm [29]), H-SSZ-24 (a zeolite with a parallel one-directional 12 MR channels with $\sigma_w = 0.70$ nm [29]) [6] and H-CIT-1 [7]. These results show that p-xylene freely moves in the 10 MR channels of H-ZSM-11 zeolite, the 12 MR channels of H-SSZ-24 and the interconnected 10/12 MR channels of CIT-1. In addition, results obtained by a molecular simulation confirm that p-xylene molecules diffuse in CIT-1 through the 10 MR and 12 MR channels [7].

Table 1
Apparent diffusivities [D_A and D_B] $\times 10^{13}$ m^2/s for the codiffusion of p-xylene (A) and o-xylene (B) in H-CIT-1 zeolite at different temperatures and $C_{p\text{-}x} = 50\%$.

Hydrocarbon	D_A ($\times 10^{13}$ m^2/s)	D_B ($\times 10^{13}$ m^2/s)	T (K)
p+o-Xylene	0.2 ± 0.04	0.2 ± 0.04	330
p+o-Xylene	0.2 ± 0.04	0.2 ± 0.04	350
p+o-Xylene	0.6 ± 0.1	1.1 ± 0.2	400
p+o-Xylene	1.6 ± 0.3	3.2 ± 0.6	425

The o-xylene diffusion critical diameter is $\sigma_m = 0.7$ nm. In that case, this molecule should moves fundamentally through the 12 MR channels. Because, as we have experimentally previously found, in zeolites with frameworks composed of 10 MR channels, o-xylene moves very slowly [5,6,8]. Molecular dynamic simulations shows that o-xylene sporadically try to go into the 10 MR channels of H-CIT-1, however, rapidly returns to the 12 MR, where this molecule stay steady for around 100 ps and afterward changes the position quickly, i.e., jump [7]. Consequently, it is possible to conclude that the interaction of the o-xylene molecule with the zeolite framework in the intersections between the 10 MR and 12 MR channels is the cause of a hopping mechanism for o-xylene, as has been found for ZSM-5 [1] and ZSM-11 [6] zeolites. Then, the o-xylene molecule, spent some time moving (around 100 ps) as a free molecule in the space around the intersections and thereafter jump [7].

In the great majority of the practical uses of nanoporous materials, mixtures of molecules are transported. Consequently, one important research activity should be the study of multicomponent diffusion. Regrettably, precise experimental studies of multicomponent diffusion in nanoporous materials are complicated [46]. Consequently, different simulation models have been proposed for the elucidation of the mechanism of mixture diffusion [10,12,15,20–22,24,46]. Nevertheless, experimental results are needed.

With the help of three different approaches, the process of multicomponent diffusion in porous materials is possible to be described. Specifically, the Fick's law, the Onsager irreversible thermodynamics, and the Maxwell–Stefan methodology [15,46,47]. The Fick's law methodology is, between them, the most frequently applied. For a binary mixture (i.e., two types of diffusing molecules: A and B) it is given by [48]:

$$\begin{aligned} J_A &= -D_{AA}\rho\nabla n_A - D_{AB}\rho\nabla n_B \\ J_B &= -D_{BA}\rho\nabla n_A - D_{BB}\rho\nabla n_B \end{aligned} \quad (2)$$

If the cross-coefficients are neglected in Eq. (2) [49]; then, for codiffusion, where the species, *A* and *B*, are diffusing in parallel, two diffusivities, $D_{AA} \approx D_A$, and, $D_{BB} \approx D_B$, can be defined. Thus, to follow the sorption kinetics, during the codiffusion experiment, it is necessary to track both components in the mixture. However, in the case of counterdiffusion, where molecule, *A*, moves "in" and molecule, *B*, moves "out", one effective diffusivity $D_e = D_A \approx D_B$ can be defined to describe the process [50,51]. Thus, to track the sorption kinetics, during the counterdiffusion experiment, it is necessary to follow only of one of the components in the mixture.

To measure these diffusivities Eq. (1) was applied. In the present cases, *D*, was substituted in Eq. (1) by: D_A and D_B, for codiffusion and by: D_e, for counterdiffusion (see Section 2.2.3). In Figs. 3 and 4, experimental kinetic curves, fitted with Eq. (1), are reported. In Tables 1–3, the resulting numerical values of the corresponding diffusivities are displayed.

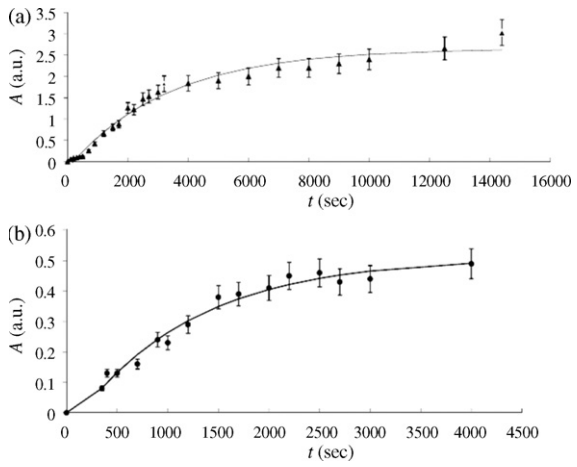

Fig. 3. Codiffusion of para- and ortho-xylene in H-CIT-1 at (a) 350 K and (b) 400 K ($C_{p\text{-}x}$ = 50%). Case where is followed the component *B*, i.e., o-xylene.

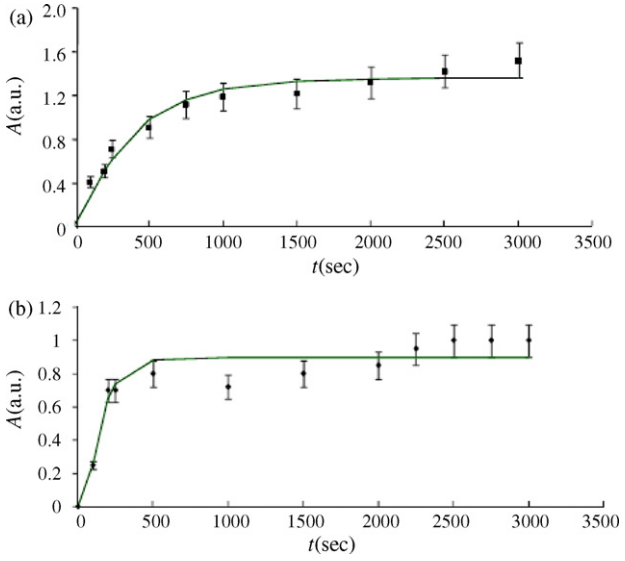

Fig. 4. Counterdiffusion of para and ortho-xylene in H-CIT-1 at (a) 375 K and (b) 400 K ($C_{p\text{-}x}$ = 50%).

Table 2
Apparent diffusivities [D_A and D_B] $\times 10^{13}$ [m^2/s] for the codiffusion of p-xylene (A) and o-xylene (B) in H-CIT-1 zeolite at 400 K and different compositions.

Hydrocarbon mixture	$C_{p\text{-}x}$ (%)	D_A ($\times 10^{13}$ m^2/s)	D_B ($\times 10^{13}$ m^2/s)
p+o-Xylene	0	–	7 ± 1
p+o-Xylene	10		1.2 ± 0.2
p+o-Xylene	20	1.3 ± 0.3	2.0 ± 0.4
p+o-Xylene	50	0.6 ± 0.1	1.1 ± 0.2
p+o-Xylene	75	1.3 ± 0.3	–
p+o-Xylene	90	1.0 ± 0.2	–
p+o-Xylene	100	1.6 ± 0.3	–

Table 3
Effective apparent diffusivity ($D_e \times 10^{13}$ m^2/s) for the counterdiffusion of the mixture p+o-xylene in H-CIT-1 zeolite at different temperatures and $C_{p\text{-}x}$ = 50% and o+p-xylene at 400 K and $C_{o\text{-}x}$ = 50%.

Hydrocarbon mixture	D_e (H-CIT-1) ($\times 10^{13}$ m^2/s)	T (K)
p+o-Xylene	0.3 ± 0.06	350
p+o-Xylene	3.8 ± 0.8	375
p+o-Xylene	3.3 ± 0.7	400
p+o-Xylene	12 ± 2	425
o+p-Xylene	0.2 ± 0.04	400

Table 4
Fickean or transport diffusion coefficients ($D \times 10^{13}$ m^2/s) for the single component diffusion of p-xylene and o-xylene in H-CIT-1 zeolite at different temperatures [7].

Hydrocarbon	D (H-CIT-1) ($\times 10^{13}$ m^2/s)	T (K)
p-Xylene	1.3 ± 0.3	350
p-Xylene	1.1 ± 0.2	375
p-Xylene	1.6 ± 0.3	400
p-Xylene	1.0 ± 0.2	425
o-Xylene	3.7 ± 0.7	350
o-Xylene	–	375
o-Xylene	7 ± 1	400
o-Xylene	15 ± 3	425

In Tables 1 and 3, the diffusivities for codiffusion and counterdiffusion at different temperatures, are reported. For the calculation of the apparent activation energy: $E^A_{a,A}$ and $E^B_{a,A}$ for codiffusion and $E_{a,A}$ for counterdiffusion, an Arrhenius type equation was applied. The calculated apparent activation energy for the codiffusion of p-xylene and o-xylene in H-CIT-1 were respectively, $E^A_{a,A} = 25 \pm 4$ kJ/mol and $E^B_{a,A} = 35 \pm 5$ kJ/mol. Additionally, the calculated apparent activation energy for the counterdiffusion of p+o-xylene mixture in H-CIT-1 was, $E_{a,A} = 34 \pm 6$ kJ/mol.

Additionally, in Table 2 the diffusivities for the codiffusion of p-xylene and o-xylene in H-CIT-1 zeolite at 400 K and different compositions are shown. It is necessary now to clarify, that during these experiments, the load of the zeolite is always the same, i.e., the number of both isomer molecules is conserved during the change of composition. Then, there is not a change in concentration.

The codiffusion experiments show, that o-xylene codiffuses at a slower rate than during single component diffusion [see Table 4 taken from Ref. [7]]. This fact is an indication of a relationship between both isomers, established during the codiffusion process through the 12 MR channels. That is, the diffusion of both molecules is coupled, since during codiffusion, the more mobile p-xylene molecules, hinders the motion of o-xylene molecules. As a consequence of this fact the apparent activation energy of both components is similar. In a molecular dynamic study of binary diffusion of para- and ortho-xylene in CIT-1, the same lowering of the rate of diffusion of o-xylene in relation to single component diffusion was found [52].

The results reported in Table 2 evidence the decrease of the diffusivity of o-xylene during codiffusion as the composition of the mixture is augmented in p-xylene. This is not a concentration effect since the total amount of both isomer molecules, that is the zeolite load, is preserved during the change of composition. Consequently, cannot be interpreted in terms of concentration changes. This is an effect of the binary mixture composition, that is, the increase in the more mobile p-xylene molecule affects the motion of o-xylene.

The counterdiffusion experiments, corresponds to two cases. One where o-xylene was previously admitted and then displaced by p-xylene (labelled as: p+o-xylene) and the second case, when p-xylene was previously admitted and displaced by o-xylene (labelled as: o+p-xylene). Both experiments were performed at the same composition ($C_{p\text{-}x}$ = 50%) and the same temperature, i.e., 400 K (see Table 3). The reported results indicate that the effective diffusivity is one order of magnitude higher for the process when o-xylene was previously admitted and then displaced by p-xylene (p+o-xylene). This is caused by the fact that the 10 MR channels are completely free for p-xylene diffusion into the zeolite. In the other case (o+p-xylene), both channels are occupied by p-xylene molecules and then the rate of diffusion for the o-xylene molecule which could only travel through the 12 MR channels, is slower. It is then possible to state, that in the p+o-counterdiffusion case, the interconnected channel structure diminish the obstruction owing to counterdiffusion, as both isomers could diffuses “in” and “out” the channel system through different pores [53].

3.3. Possibility of molecular traffic control in a zeolite with 10 MR/12 MR interconnected channels

Molecular traffic control (MTC) is an especially complicated effect, which is also difficult to clearly define [21]. Then, previous to the discussion of the possibility of molecular traffic control in the system studied here, we will comment different definitions of the MTC concept proposed in the specialized literature. The original MTC concept, suggested, that it is possible to improves the operation of a zeolite catalyst by directing the reactive and the reaction products molecules through different paths [19,54,55]. To be precise, in some instances, in a zeolite or other microporous crystalline material, the molecules of the reactants will enter through one kind of channel and the molecules of the reaction products will leave the reaction site through a different channel [21]. It is then possible to state that, during MTC, the interconnected channel structure diminish the obstruction owing to counterdiffusion, as both molecules could diffuse in and out of the channel system through different pores [53]. In other words, during MTC takes place the following effect: molecules are able to diffuse in a channel system with pores of different sizes, along different paths, in such way, that the small molecules diffuses through the small channels and the large through the large channels with the consequence that counterdiffusion is minimized [55]. Finally, it is also considered that the cause of MTC is the mutual correlation in the motion of a multicomponent fluid through two types of pores [56].

In our case, the zeolite with a 10 MR and 12 MR interconnected channels tested was the H-CIT-1 zeolite, which shows a CON framework [29]. In this structure, the codiffusion experiments demonstrate that the movement of both isomers has a mutual correlation. This is a necessary condition for MTC. But, in the present case is not enough, to prove the existence of MTC. Then, it is possible to state, following our codiffusion data, that a certain manifestation of molecular traffic control exist. However, the counterdiffusion experiment, is more informative, since it clearly shows that in the interconnected channel structure of the CIT-1 zeolite, the para- and ortho-xylene molecules are capable to diffuse along different pores with the consequence that counterdiffusion is minimized [55]. Since, as p-xylene could freely diffuse, "in" and "out" the zeolite through the 10 MR channels which are blocked for o-xylene molecules, then, the p-xylene motion is not hindered by o-xylene molecules during p+o counterdiffusion. As a result, it is feasible to affirm that, a molecular traffic control is taking place.

4. Conclusions

With the FTIR method, the apparent diffusivities in two component codiffusion and counterdiffusion experiments in the intersecting two-directional 10 MR and 12 MR channel system of zeolite H-CIT-1, were measured. The values of the diffusivities in the codiffusion and counterdiffusion experiments were calculated. The mechanisms of codiffusion and counterdiffusion were discussed. A relationship in the motion of both isomers, during codiffusion and counterdiffusion, was observed. During codiffusion, the p-xylene molecule slows down the motion of o-xylene. Throughout, the p+o counterdiffusion case, one molecule, p-xylene, moves "in", and the other molecule, o-xylene, moves "out"; then, since the 10 MR channels are blocked for o-xylene molecules, are free for p-xylene motion; taking place a molecular traffic control effect.

Nomenclature

a	spherical shape crystal diameter [μm]
A	absorbance of the IR peak (in arbitrary units [a.u.])
$C_{p\text{-}x}$	gas phase composition of p-xylene [%]
$C_{o\text{-}x}$	gas phase composition of o-xylene [%]
D	Fickean diffusion coefficient or chemical diffusion coefficient for single component diffusion [m^2/s]
$D_{\alpha\beta}$	Fickean diffusivities for multicomponent diffusion [m^2/s]
D_e	effective diffusivity in counterdiffusion [m^2/s]
D_A	$D_{AA} \approx D_A$, diffusivity coefficient of component A in the case of codiffusion [m^2/s]
D_B	$D_{BB} \approx D_B$, diffusivity coefficient of component B in the case of codiffusion [m^2/s]
D_e	$D_e = D_A \approx D_B$, effective diffusivity in counterdiffusion [m^2/s]
$E^A_{a,A}$	apparent activation energy for the codiffusion of component A [kJ/mol]
$E^B_{a,A}$	apparent activation energy for the codiffusion of component B [kJ/mol]
$E_{a,A}$	apparent activation energy for counterdiffusion [kJ/mol]
M_t	amount of sorbate taken at time, t [kg]
M_∞	equilibrium amount of sorption [kg]
n_α	adsorbed phase concentration [mol/kg]
r	radius of the zeolite crystallite [μm]

Greek symbols

β	time constant [s^{-1}]
σ_m	diffusion critical diameter of a molecule [nm]
σ_w	maximum window, or channel diameter of a crystalline microporous material [nm]
ρ	particle density [kg/m^3]

Acknowledgments

The authors acknowledges the financial support provided by the "Consejo Superior de Investigaciones Científicas (CSIC)" of Spain at the "Instituto de Tecnología Química (ITQ)", in Valencia, Spain, where the experimental part of the present research was carried out. The authors also thank Dr. Avelino Corma for many helpful discussions and sponsorship, Dr. Amparo Mifsud for the SEM study of the H-CIT-1 sample and support, and Dr. Raul Lobos for providing the CIT-1 sample. Besides, one of the authors (RRM), acknowledges that the final steps in the preparation of the present paper were carried out with the financial support provided by the US Department of Energy through the Massey Chair project at University of Turabo.

References

[1] J. Karger, D.M. Ruthven, Diffusion in Zeolites and other Microporous Solids, J. Wiley and Sons, New York, 1992.
[2] R. Roque-Malherbe, Adsorption and Diffusion in Nanoporous Materials, CRC Press, Boca Raton, Florida, 2007.
[3] R. Roque-Malherbe, The Physical Chemistry of Materials: Energy and Environmental Applications, CRC Press, Boca Raton, Florida, 2009.
[4] W. Niessen, H.G. Harge, Stud. Surf. Sci. Catal. 60 (1991) 213–221.
[5] R. Roque-Malherbe, R. Wendelbo, A. Mifsud, A. Corma, J. Phys. Chem. 99 (1995) 14064–14071.
[6] R. Roque-Malherbe, V. Ivanov, Micropor. Mesopor. Mater. 47 (2001) 25–38.
[7] G. Sastre, N. Raj, C. Richard, C. Catlow, R. Roque-Malherbe, A. Corma, J. Phys. Chem. B 102 (1998) 3198–3209.
[8] R. Wendelbo, R. Roque-Malherbe, Micropor. Mater. 10 (1997) 231–246.
[9] J. Valyon, G. Onyestyak, L.V.C. Rees, Langmuir 16 (2000) 1331–1336.
[10] J. Karger, Single-File Diffusion in Zeolites, in Molecular Sieves-Science and Technology Series, vol. 7, Springer-Verlag, Berlin-Heidelberg, 2008, pp. 329–366.
[11] D.F. Plant, G. Maurin, R.G. Bell, J. Phys. Chem. B 111 (2007) 2836–2844.
[12] A. Gupta, R.Q. Snurr, J. Phys. Chem. B 109 (2005) 1822–1833.
[13] P. Demontis, F.G. Pazzona, G.B. Suffritti, J. Phys. Chem. B 110 (2006) 13554–13559.
[14] H. Ramanan, S.M. Auerbach, M. Tsapatsis, J. Phys. Chem. B 108 (2004) 17171–17178.
[15] D.S. Sholl, Acc. Chem. Res. 39 (2006) 403–411.
[16] M.S. Post, Stud. Surf. Sci. Catal. 58 (1991) 391–443.
[17] A. Bhan, E. Iglesia, Acc. Chem. Res. 41 (2008) 559–567.

[18] A. Corma, Micropor. Mesopor. Mater. 21 (1998) 487–495.
[19] G. Derouane, Z. Gabelica, J. Catal. 65 (1980) 486–489.
[20] P. Bruer, A. Brzank, J. Karger, J. Phys. Chem. B 107 (2003) 1821–1831.
[21] L.A. Clark, G.T. Ye, R.Q. Snurr, Phys. Rev. Lett. 84 (2000) 2893–2896.
[22] P. Brauer, S. Fritzsche, J. Karger, G. Schutz, S. Vasenkov, Lect. Notes Phys. 634 (2004) 89–125.
[23] J. Kärger, Ind. Eng. Chem. Res. 41 (2002) 3335–3340.
[24] R. Harish, D. Karevski, G.M. Schütz, J. Catal. 253 (2008) 191–199.
[25] P.M.M. Blawhoff, J.W. Gosselnik, E.P. Kieffer, S.T. Tie, W.H.J. Stork, in: J. Weitkamp, L. Puppe (Eds.), Catalysis and Zeolites: Fundamentals and Applications, Spinger-Verlag, Berlin, 1999, pp. 437–538.
[26] W.E. Farneth, R.J. Gorte, Chem. Rev. 95 (1995) 615–635.
[27] K. Tanabe, W.F. Holderich, Appl. Catal. A 181 (1999) 399–434.
[28] L. Yang, K. Trafford, O. Kresnawahjuesa, J. Sepa, R.J. Gorte, D. White, J. Phys. Chem. B 105 (2001) 1935–1942.
[29] Ch. Baerlocher, W.M. Meier, D.M. Olson, Atlas of Zeolite Framework Types, 5th ed., Elsevier, Amsterdam, 2001.
[30] R. Castañeda, A. Corma, V. Forns, F. Rey, J. Rius, J. Am. Chem. Soc. 125 (2003) 7820–7821.
[31] R.F. Lobo, M. Pan, I. Chan, H.X. Li, R.C. Medrud, S.I. Zones, P.A. Crozier, M.E. Davis, Science 262 (1993) 1543–1546.
[32] R.F. Lobo, M. Pan, I. Chan, R.C. Medrud, S.I. Zones, P.A. Crozier, M.E. Davis, J. Phys. Chem. 98 (1994) 12040–12052.
[33] R.F. Lobo, M.E. Davis, Micropor. Mater. 3 (1994) 61–69.
[34] R.F. Lobo, M.E. Davis, J. Am. Chem. Soc. 117 (1995) 3766–3779.
[35] R.F. Lobo, PhD. Thesis, California Institute of Technology, Pasadena, CA, 1994.
[36] A. Santoro, J. Res. Natl. Instit. Stand. Technol. 106 (2001) 921–952.
[37] J. Crank, The Mathematics of Diffusion, 2nd ed., Oxford University Press, Oxford, 1975.
[38] PeakFit®, Program System, Seasolve Software Inc., Framingham, Massachusetts, 2003.
[39] A. Micke, M. Bulow, Zeolites 12 (1992) 216–217;
A. Micke, M. Bulow, Stud. Surf. Sci. Catal. 84 (1994) 1315–1321.
[40] J. Karger, P. Vasenkow, in: S.M. Auerbach, K.A. Carrado, P.K. Dutta (Eds.), Handbook of Zeolite Science and Technology, Marcell Dekker, Inc., New York, 2003, pp. 341–422.
[41] J. Wei, Ind. Eng. Chem. Res. 33 (1994) 2467–2472.
[42] R. Lobo, in: S.M. Auerbach, K.A. Carrado, P.K. Dutta (Eds.), Handbook of Zeolite Science and Technology, Marcell Dekker, Inc., New York, 2003, pp. 65–89.
[43] G. Sastre, Ph.D. Thesis, University of Valencia, 1995.
[44] D. Barthomeuf, A. Mallmann, Ind. Eng. Chem. Res. 29 (1990) 1435–1438.
[45] R. Roque-Malherbe, F. Diaz-Castro, J. Mol. Catal. A 280 (2008) 194–202.
[46] D.S. Sholl, Langmuir 22 (2006), 3707–3714.
[47] D. Pashek, R. Krishna, Langmuir 17 (2001) 247–254.
[48] Y. Wang, M.D. LeVan, Ind. Eng. Chem. Res. 46 (2007) 2141–2154.
[49] J. Karger, M. Bulow, Chem. Eng. Sci. 30 (1975) 893–896.
[50] D.M. Ruthven, Principles of Adsorption and Adsorption Process, J. Wiley and Sons, New York, 1984.
[51] W.R. Qureshi, J. Wei, J. Catal. 126 (1990) 147–172.
[52] G. Sastre, A. Corma, C.R.A. Catlow, Top. Catal. 9 (1999) 215–224.
[53] W. Rudziski, J. Narkiewicz-Michaek, P. Szabelski, A.S.T. Chiang, Langmuir 13 (1997) 1095–1103.
[54] J. Kärger, R. Valiullin, S. Vasenkov, New J. Phys. 7 (2005) 15 (www.njp.org).
[55] E.G. Derouane, A Molecular View of Heterogeneous Catalysis: Proceedings of the First Francqui Colloquium, Brussels, February, 1996, De Boeck Universite Press, 1998, pp. 5–27.
[56] D. Dubbeldam, E. Beerdsen, S. Calero, B. Smit, J. Phys. Chem. B 110 (2006) 3164–3172.